ORIGINAL RESEARCH

Restriction of H1N1 influenza virus infection by selenium nanoparticles loaded with ribavirin via resisting caspase-3 apoptotic pathway

Zhengfang Lin[1,*]
Yinghua Li[1,*]
Guifang Gong[2]
Yu Xia[1]
Changbing Wang[1]
Yi Chen[1]
Liang Hua[1]
Jiayu Zhong[1]
Ying Tang[1]
Xiaomin Liu[1]
Bing Zhu[1]

[1]Department of Center Laboratory, Guangzhou Women and Children's Medical Center, Guangzhou Medical University, Guangzhou, Guangdong, People's Republic of China; [2]Department of Obstetrics Gynecology, Guangzhou Women and Children's Medical Center, Guangzhou Medical University, Guangzhou, People's Republic of China

*These authors contributed equally to this work

Correspondence: Yinghua Li; Bing Zhu
Department of Center Laboratory, Guangzhou Women and Children's Medical Center, Guangzhou Medical University, No 318 Renminzhong Road, Yuexiu District, Guangzhou 510120, People's Republic of China
Tel +86 20 8133 0740
Fax +86 20 8188 5978
Email hualei_1314@hotmail.com; zhubing2016@hotmail.com

Introduction: Ribavirin (RBV) is a broad-spectrum antiviral drug. Selenium nanoparticles (SeNPs) attract much attention in the biomedical field and are used as carriers of drugs in current research studies. In this study, SeNPs were decorated by RBV, and the novel nanoparticle system was well characterized. Madin-Darby Canine Kidney cells were infected with H1N1 influenza virus before treatment with RBV, SeNPs, and SeNPs loaded with RBV (Se@RBV).

Methods and results: MTT assay showed that Se@RBV nanoparticles protect cells during H1N1 infection in vitro. Se@RBV depressed virus titer in the culture supernatant. Intracellular localization detection revealed that Se@RBV accumulated in lysosome and escaped to cytoplasm as time elapsed. Furthermore, activation of caspase-3 was resisted by Se@RBV. Expressions of proteins related to caspase-3, including cleaved poly-ADP-ribose polymerase, caspase-8, and Bax, were downregulated evidently after treatment with Se@RBV compared with the untreated infection group. In addition, phosphorylations of phosphorylated 38 (p38), JNK, and phosphorylated 53 (p53) were inhibited as well. In vivo experiments indicated that Se@RBV was found to prevent lung injury in H1N1-infected mice through hematoxylin and eosin staining. Tunel test of lung tissues present that DNA damage reached a high level but reduced substantially when treated with Se@RBV. Immunohistochemical test revealed an identical result with the in vitro experiment that activations of caspase-3 and proteins on the apoptosis pathway were restrained by Se@RBV treatment.

Conclusion: Taken together, this study elaborates that Se@RBV is a novel promising agent against H1N1 influenza virus infection.

Keywords: nanomaterials, H1N1 influenza virus, rivabirin, apoptosis, caspase-3

Introduction

Influenza breaks out every year and causes severe infection in the respiratory system.[1,2] The novel H1N1 influenza pandemic that erupted in North America caused more than 575,400 deaths in 2009.[3] Vaccines and antiviral drugs are the main methods to prevent and control influenza. Because of the variation of influenza virus, application of vaccines is severely circumscribed. Current therapeutic strategies for influenza include the M2 ion channel inhibitors, neuraminidase inhibitors, and broad-spectrum antiviral RNA polymerase inhibitors. Amantadine, oseltamivir, and zanamivir, the main M2 ion channel inhibitor and neuraminidase inhibitors that once had a remarkable effect on influenza virus infection, have been reported increasingly for their resistance.[4–6] Development of new drugs and drug combinations is focused on in medicine. Ribavirin (RBV) is a triazole compound and nucleoside analog. As an RNA polymerase inhibitor, RBV is a well-characterized and broad-spectrum antiviral drug against various RNA and DNA viruses, including influenza A and influenza B viruses.[7] It was approved by

the American Food and Drug Administration for treatment against influenza virus or respiratory syncytial virus infection through nebulizer inhalation in 1986 and hepatitis C virus infection combined with interferon in 2001.[8]

Nanomaterials have been studied or applied as carriers of drugs in the biomedical field because of their special physical and chemical properties compared with normal materials, such as the small particle size that contributes to the stable nanostructure and enables easy entrance into cells.[9,10] It has been reported that silver nanoparticles loaded with paclitaxel enhance apoptosis of HepG2 cancer cells compared with paclitaxel alone.[11] Gold nanoparticles are used to deliver chemotherapeutic drugs in research studies because of their remarkable properties, including high surface-area-to-volume ratio, surface plasmon resonance, and so forth.[12] Mesoporous silica nanoparticles loaded with doxorubicin exhibit higher intracellular drug release in cancer cells.[13] Compared with these elements, selenium nanoparticles (SeNPs) have their own characteristics against virus infection. First, selenium status may affect the function of cells of both innate and adaptive immunity. It has been reported that selenium deficiency is supposed to be related to virus infection, including coxsackie virus and human immunodeficiency virus.[14,15] Selenium supplementation in healthy human adults with marginal selenium status results in both beneficial and detrimental effects on cellular immunity to flu caused by influenza virus.[16] Sodium selenite suppresses hepatitis B virus transcription and replication in vitro.[17] Furthermore, SeNPs were used to induce robust Th1 cytokine pattern with hepatitis B virus vaccination.[18] Besides, SeNPs showed anti-type-1 dengue virus activity by depressing cytopathic effect.[19] Our previous studies proved that SeNPs loaded with oseltamivir or amantadine can, respectively, inhibit apoptosis induced by influenza virus infection in vitro.[20,21]

It has been reported that viruses induce apoptosis through caspase-3 activation.[22–24] Caspase-3 is the primary executioner of programmed cell death. It is directly or indirectly responsible for the cleavage of many proteins and caspases involved in apoptosis.[25] It is activated when cleaved into two protein fragments. Cleaved caspase-3 is responsible for the proteolytic cleavage of many critical proteins. Here, RBV was carried by SeNPs, making a new nanoparticle drug system that enters the cells more effectively. Then, the antiviral activity against H1N1 influenza virus of the nano system was detected via cell viability assay and viral titer test in vitro, followed by lungs injury detection. Finally, the relationship between the antiviral activity and caspase-3 apoptotic pathway was explored in both in vitro and in vivo experiments.

Materials and methods
Materials
Madin-Darby Canine Kidney (MDCK) cells were bought from American Type Culture Collection (Manassas, VA, USA). A/Guangdong/1/2009 H1N1 influenza virus was donated by the Guangzhou Institute of Respiratory Disease. Dulbecco's Modified Eagle's Medium (DMEM) and fetal bovine serum (FBS) were gained from Thermo Fisher Scientific (Waltham, MA, USA). L-1-Tosylamido-2-phenylethyl chloromethyl ketone (TPCK), thiazolyl blue tetrazolium bromide (MTT), Na_2SeO_3, ascorbic acid (VC), RBV, lyso tracker, 4′6-diamidino-2-phenyindole (DAPI), and coumarin-6 from Sigma-Aldrich Co. (St Louis, MO, USA) were used in the study. A one-step reverse transcription polymerase chain reaction (RT-PCR) kit was acquired from Takara (Kyoto, Japan). Primers and probe were synthetized by Sangon Biotech (Shanghai, People's Republic of China). Caspase-3 activity assay kit and tunel detection kit were purchased from Beyotime (Jiangsu, People's Republic of China). Cleaved caspase-3, cleaved poly-ADP-ribose polymerase (PARP), caspase-8, phosphorylated p53 (p-p53), Bax, phosphorylated p38 (p-p38), phosphorylated Jun-amino-terminal kinase (p-JNK), and β-actin monoclone antibodies were supplied by Cell Signaling Technology (Danvers, MA, USA). Dimethylbenzene, 3% hydrogen peroxide (H_2O_2), 3,3′-diaminobenzidine (DAB), and mounting medium were bought from GBCBIO Technologies (Guangdong, People's Republic of China).

Synthesis of SeNPs loaded with RBV (Se@RBV)
About 0.25 mL of 0.1 M Na_2SeO_3 solution and 2 mL of 0.5 mM VC solution were dropped into 22.75 mL ultrapure water. After stirring for 30 minutes, RBV was added, followed by a dialysis for 24 hours.[26] Concentration of Se@RBV was detected using inductively coupled plasma-atomic emission spectrometry. The $SeNP_S$ and Se@RBV samples were stored at 4°C.

Characterization of Se@RBV
Morphology of Se@RBV was observed by a transmission electron microscopy (TEM). Elemental composition of Se@RBV was detected by an energy-dispersive X-ray spectroscopy (EDX). Size distribution and zeta potential of Se@RBV were determined by a zetasizer analyzer.[27]

Cell culture and virus infection
MDCK cells were cultured in DMEM with 10% FBS, 100 U/mL penicillin, and 50 U/mL streptomycin at 37°C with

5% CO_2. MDCK cells were infected with H1N1 influenza virus and 50% tissue culture infective dose ($TCID_{50}$) was calculated.[28] In brief, cells were plated for 24 hours and then adsorbed with H1N1 virus for 2 hours. The supernatant was replaced with DMEM containing 2 µg/mL TPCK-treated trypsin. The $TCID_{50}$ was calculated using the Reed–Muench method.[29] H1N1 virus was used for in vitro study at the titer of 100 $TCID_{50}$/mL, 1000 $TCID_{50}$/mL for in vivo experiments.

Cell viability test

Cytotoxicity of Se@RBV was detected by MTT assay.[30] MDCK cells infected by H1N1 virus were treated with 15.6 µM SeNPs and 40 µg/mL RBV and Se@RBV containing 15.6 µM SeNPs and 40 µg/mL RBV, respectively, for 24 hours. MTT solution was added at a final concentration of 0.5 mg/mL after 48 hours. Solution in the wells was sucked away 4 hours later, and 150 µL dimethyl sulfoxide was added. The absorbance values were recorded at 570 nm 20 minutes later.

Viral proliferation

RNA level of H1N1 virus was tested by RT-PCR. RNA was extracted and amplification was performed with a one-step RT-PCR kit. Primers were as follows: H1N1 forward primer 5′ CTCAGCAAATCCTACATTA 3′ and reverse primer 5′ TAGTAGATGGATGGTGAAT 3′. Sequence of the probe was CCATAGCACGAGGACTTCTT,[31] GAPDH forward primer 5′ CGCCAAGAAGGTGATCATTTC 3′, and reverse primer 5′ CAGGAGGCGTTCGAGATGAC 3′.

Intracellular localization of Se@RBV

MDCK cells cultured in dishes were treated with lyso tracker for 90 minutes. DAPI and coumarin-6 labeled Se@RBV were added for various time periods of incubation.[32] The images were again analyzed and analyzed by a fluorescence microscope.

Caspase-3 activity

Caspase-3 activity was mensurated using a caspase-3 activity detection kit.[33]

Western blot

Then, the cells were lysed with radioimmunoprecipitation assay buffer.[34] The lysates were separated by sodium dodecyl sulfate-polyacrylamide gel. Bands on polyvinylidene difluoride membranes were immunoblotted with primary antibodies, including cleaved caspase-3, cleaved PARP, caspase-8, p-p53, Bax, p-p38, p-JNK and β-actin monoclone antibodies, and secondary antibodies. Images were visualized on a Tanon gel imaging system.

Animal infection and treatment

Fifteen female BALB/c mice aged 4–6 weeks (Animal Experiment Center of Guangdong Province, People's Republic of China) were randomly divided into five groups: physiological saline group that without infection and treatment was as control; mock group was as H1N1 virus control; RBV group was treated with RBV post infection; SeNPs group was treated with SeNPs and Se@RBV group was treated with SeNPs loaded with RBV. All mice were anesthetized with 10% chloral hydrate at a dose of 3 µL/g through intraperitoneal injection. Then, the control group was treated with 20 µL physiological saline by nasal dripping, while the other four groups were treated with 20 µL H1N1 virus at a 1,000 $TCID_{50}$/mL titer by nasal dripping as well.[35,36] After 24 hours, RBV, SeNPs and Se@RBV that contained 20 µg RBV and 50 nmol SeNPs were administered to anesthetized mice, respectively, via intranasal absorption every 24 hours thereafter for a total of three times. Clinical symptoms of the mice were observed, and then the mice were executed by cervical dislocation after anesthesia with chloral hydrate on the 14th day from which treatment was given last. The lungs were extracted, affused with physiological saline, and fixed in paraformaldehyde before hematoxylin and eosin (H&E) staining, tunel test, and immunohistochemistry staining were done. All mice experiments were approved and guided by the ethics committee of Guangzhou Medical University and Experimental Animal Center of Guangzhou Medical University.

H&E staining, tunel test, and immunohistochemistry

The lungs were fixed in 4% paraformaldehyde for 24 hours, dehydrated in a graded ethanol series, and embedded in paraffin. Sections were embedded in wax and cut into 5 µm slices for H&E staining, tunel test, and immunohistochemistry.[37] For the tunel test, slices were labeled with tunel reaction mixture and DAPI. Green fluorescence stood for positive. For immunohistochemistry, slices were dewaxed with dimethylbenzene for 15 minutes and rehydrated with alcohol for 40 minutes before antigen retrieval. After quenching with 3% H_2O_2 and blocking, the slices were incubated with cleaved caspase-3, cleaved PARP, p-p53, p-p38, and p-JNK antibodies, respectively, at 4°C overnight. Followed by incubation with secondary antibodies and coloration

with DAB, the slices were dehydrated and treated with mounting medium before observation under a Leica digital microscope.

Statistical analysis

GraphPad Prism 5.0 software (GraphPad Software, Inc., La Jolla, CA, USA) was used for data analysis.[38] Two-tailed Student's *t*-test and a one-way analysis of variance were used to evaluate the significance of the data. Differences were considered statistically significant at $P < 0.05$ (*) or $P < 0.01$ (**).[39]

Results and discussion
Preparation and characterization of Se@RBV

As shown in the TEM images in Figure 1A, SeNPs and Se@RBV appeared monodisperse and spherical. Moreover, the diameter of SeNPs was 200 nm, while that of Se@RBV <100 nm. Size distribution in Figure 1C confirmed that the average sizes of Se@RBV and SeNPs were 65 nm

and 100 nm, respectively. When decorated with RBV on the surface, the surface-free energy of SeNPs decreased and the nanoparticles became more stable. Thus, the diameter of Se@RBV is smaller than SeNPs alone. The particle size of Se@RBV contributed to the stable nanostructure, which made it propitious to pass through the cytomembrane. Surface elemental composition analysis was carried out by EDX. Figure 1B reveals a strong signal of Se atom (91.5%), C atom (7.2%), O atom (1.1%), and N atom (0.2%). The presence of O atom indicated that RBV had conjugated to the surface of SeNPs. As shown in Figure 1D, the zeta potential of SeNPs alone was −25 mV and decreased to −10 mV after carrying RBV, explaining the higher stability of Se@RBV.

Cells viability and viral proliferation with Se@RBV

MDCK cells were infected with H1N1 virus and were subsequently untreated or treated with RBV, SeNPs, or Se@RBV. Cytotoxic effect of MDCK cells was detected by MTT assay. As Figure 2A indicated, cell viability without treatment after
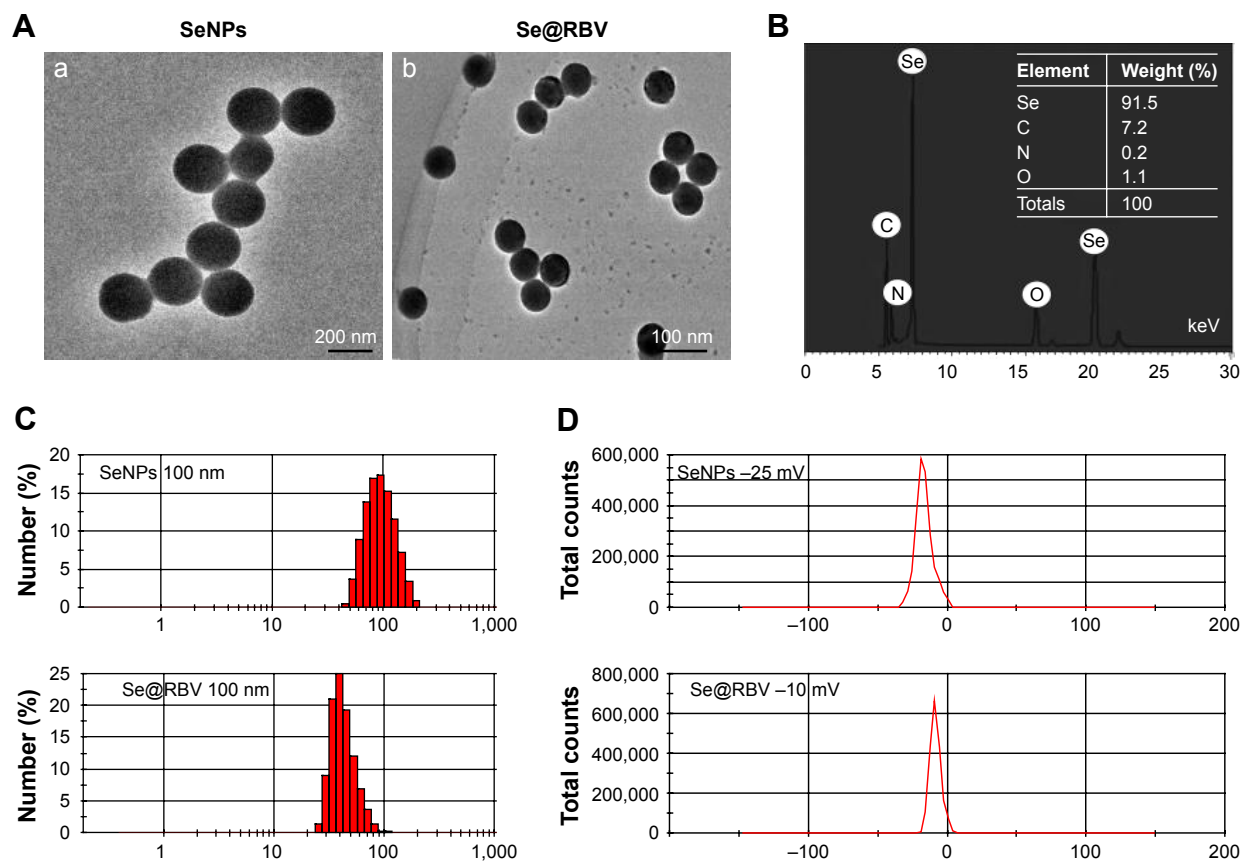

Figure 1 Characterization of SeNPs and Se@RBV.
Notes: (**A**) TEM images of SeNPs (a) and Se@RBV (b). (**B**) Elemental composition analysis of Se@RBV by EDX. (**C**) Size distributions of SeNPs and Se@RBV. (**D**) Zeta potentials of SeNPs and Se@RBV.
Abbreviations: EDX, energy-dispersive X-ray spectroscopy; RBV, ribavirin; SeNPs, selenium nanoparticles; Se@RBV, SeNPs loaded with RBV; TEM, transmission electron microscopy.
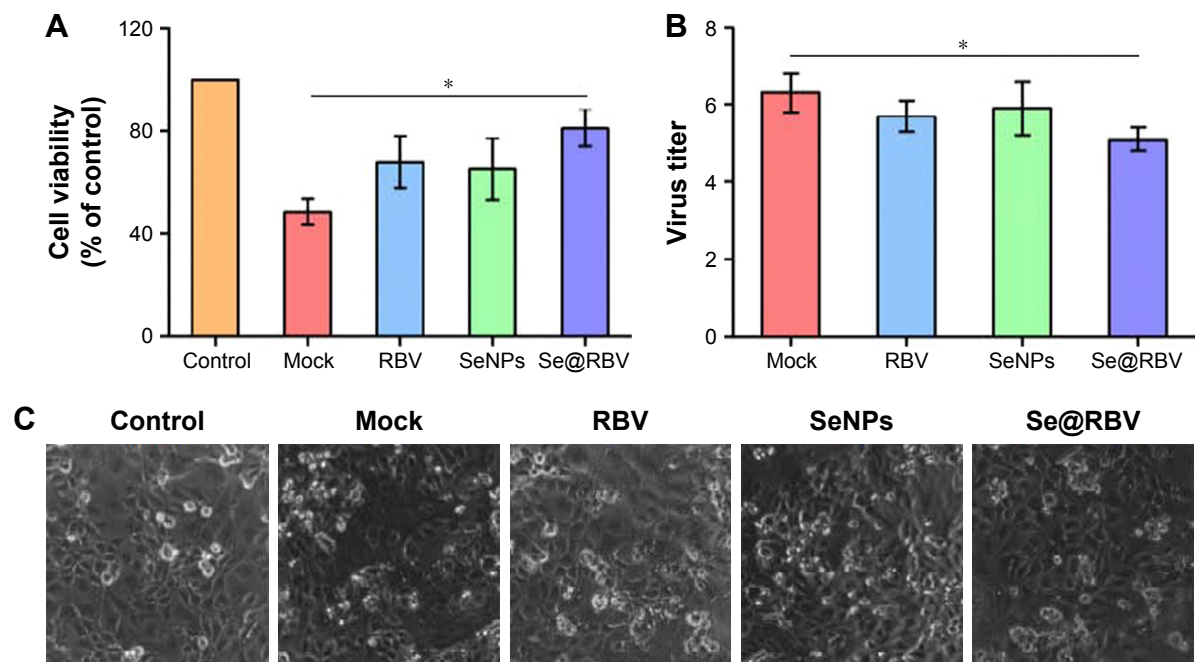
Figure 2 Cell viability and viral proliferation.
Notes: MDCK cells infected with H1N1 virus were untreated (Mock) or treated with RBV, SeNPs, and Se@RBV for 48 hours. Cells without infection and treatment were performed as control. Cell viability (**A**) and virus titer of the culture supernatant (**B**) were detected. Cytopathic effect was observed under a microscope (**C**). *$P < 0.05$.
Abbreviations: MDCK, Madin-Darby Canine Kidney; RBV, ribavirin; SeNPs, selenium nanoparticles; Se@RBV, SeNPs loaded with RBV.

infection was 48.4%, and cells treated with RBV or SeNPs achieved a viability of 68.5% and 65.2%, respectively. In addition, cells treated with Se@RBV achieved a significant viability of 80.6%. These data indicated that the antiviral activity of RBV effectively got strengthened when coated by SeNPs. RNA level of H1N1 was tested. As was displayed in Figure 2B, cells treated with Se@RBV after infection got a lowest titer level than RBV or SeNPs alone, suggesting that RBV was more effective when loaded by SeNPs. In Figure 2C, cells infected with H1N1 virus without treatment showed an enlarged intercellular space, cell swelling, and lysis. The cytopathic effect weakened when treated with Se@RBV. These assays presented that Se@RBV effectively resisted proliferation of H1N1 virus.

Intracellular localization of Se@RBV

Endocytosis against nanoparticles is significant to the transmission study of drugs loaded with nanosystems. As Figure 3 shows, the green coumarin-6 labeled Se@RBV accumulated on MDCK cells membrane and moved to lysosomes labeled by red lyso tracker, presenting yellow or purple of the overlap sites. Approximately 60 minutes later, Se@RBV escaped from lysosomes and released into the cytoplasm. Chen et al[17] have reported that SeNPs loaded polysaccharide shuttled across the cell membrane in 1 hour

accumulated gradually in lysosomes and dispersed in the cytoplasm. This result is coincident with this study.[40] The detection suggested that Se@RBV targeted lysosomes for subsequent cellular actions.

Restriction on caspase-3 activation in vitro

Apoptosis is induced during H1N1 virus infection.[41] MDCK cells were treated with RBV, SeNPs, or Se@RBV after H1N1 virus infection. Activity of caspase-3 was detected, and expression of cleaved caspase-3 or cleaved PARP was investigated. As reflected in Figure 4, caspase-3 activity of cells infected by H1N1 virus without treatment was 352% of the control group in which cells were uninfected, while the Se@RBV-treated group markedly reduced to 208%, compared with 262% of the RBV-treated group and 304% of the SeNPs group. It suggested that H1N1 virus probably induced apoptosis through caspase-3 and was effectively suppressed by Se@RBV. In addition, expression of caspase-8 protein was decreased and that of cleaved caspase-3 and cleaved PARP increased after H1N1 infection. When treated with Se@RBV, changes of the three turned weak. These results suggested that Se@RBV inhibited apoptosis by regulating caspase-8, caspase-3, and PARP proteins. Caspase-8 is an apoptosis initiator. Activated caspase-8 cleaves apoptosis executioners, such as caspase-3, caspase-6, and caspase-7.[42]
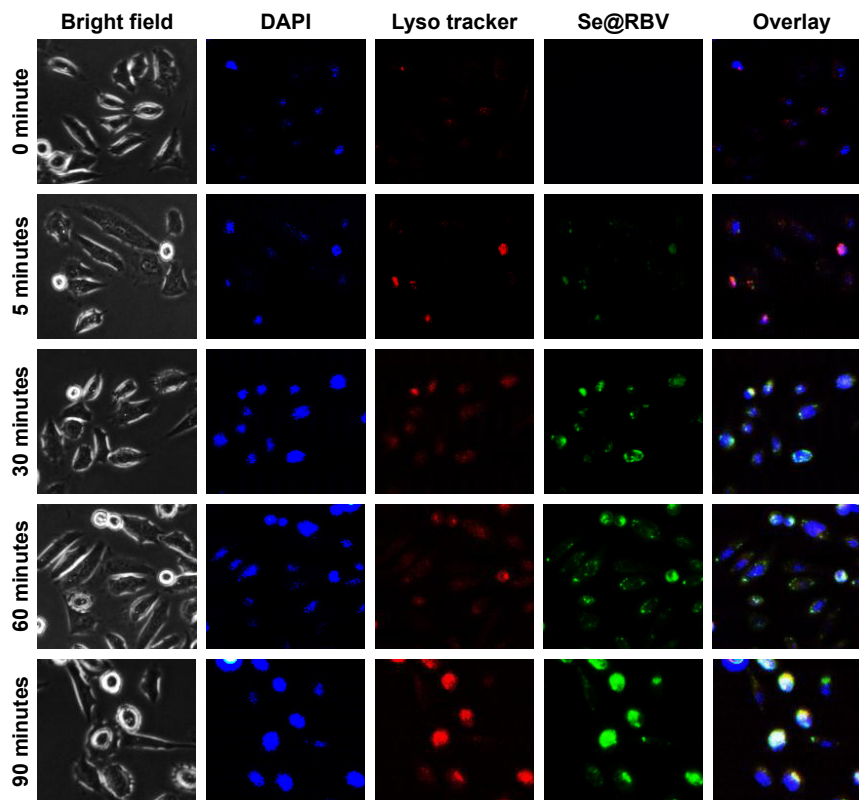
Figure 3 Intracellular localization of Se@RBV.
Notes: MDCK cells were treated with coumarin-6-loaded Se@RBV for 90 minutes and stained with lyso tracker for lysosome and DAPI for nucleus. Cells were observed under a fluorescent microscope at a different time.
Abbreviations: DAPI, 4′6-diamidino-2-phenyindole; MDCK, Madin-Darby Canine Kidney; RBV, ribavirin; SeNPs, selenium nanoparticles; Se@RBV, SeNPs loaded with RBV.

Cleaved caspase-3 is responsible for the proteolytic cleavage of many critical proteins, such as the PARP. Cleavage of PARP facilitates cellular disassembly and serves as a marker of apoptosis.[43] It could be inferred that Se@RBV restrained

Figure 4 Restriction on caspase-3 activation in vitro.
Notes: MDCK cells infected with H1N1 virus were untreated (Mock) or treated with RBV, SeNPs, and Se@RBV for 48 hours. Cells without infection and treatment were performed as control. Caspase-3 activity was checked and expressions of proteins related to caspase-3 activation were detected. *P<0.05 and **P<0.01.
Abbreviations: MDCK, Madin-Darby Canine Kidney; RBV, ribavirin; SeNPs, selenium nanoparticles; Se@RBV, SeNPs loaded with RBV.

the caspase-3-mediated apoptosis pathway by inhibiting the activation of caspase-8.

Inhibition of apoptosis signaling pathways

MDCK cells infected with H1N1 virus were treated with RBV, SeNPs, and Se@RBV for 24 hours. Proteins related to apoptosis signaling pathways were detected. As was mentioned earlier, Se@RBV inhibited caspase-3-mediated mitochondrial apoptosis. Bax plays a key role in the apoptosis during mitochondrial stress. It enhances membrane permeability and helps the activation of caspase pathways, such as caspase-3.[44] As shown in Figure 5A, H1N1 virus infection led to an increased expression of Bax protein. After treatment with Se@RBV, the expression was downregulated. In addition, expression of p-p53 had an identical variation tendency with Bax. P53 is activated after phosphorylation. Activated p53 affects apoptosis by regulating Bcl-2 and Bax gene. As an activator of transcription of Bax, p53 benefits the expression of the protein and promotes the apoptosis process after phosphorylation.[45] The results suggested that Se@RBV might regulate the expression of Bax through attenuating the expression of p53 protein. Meanwhile, Se@RBV restrained
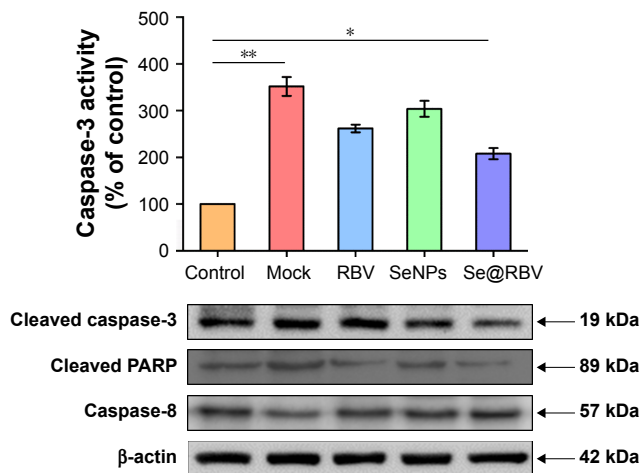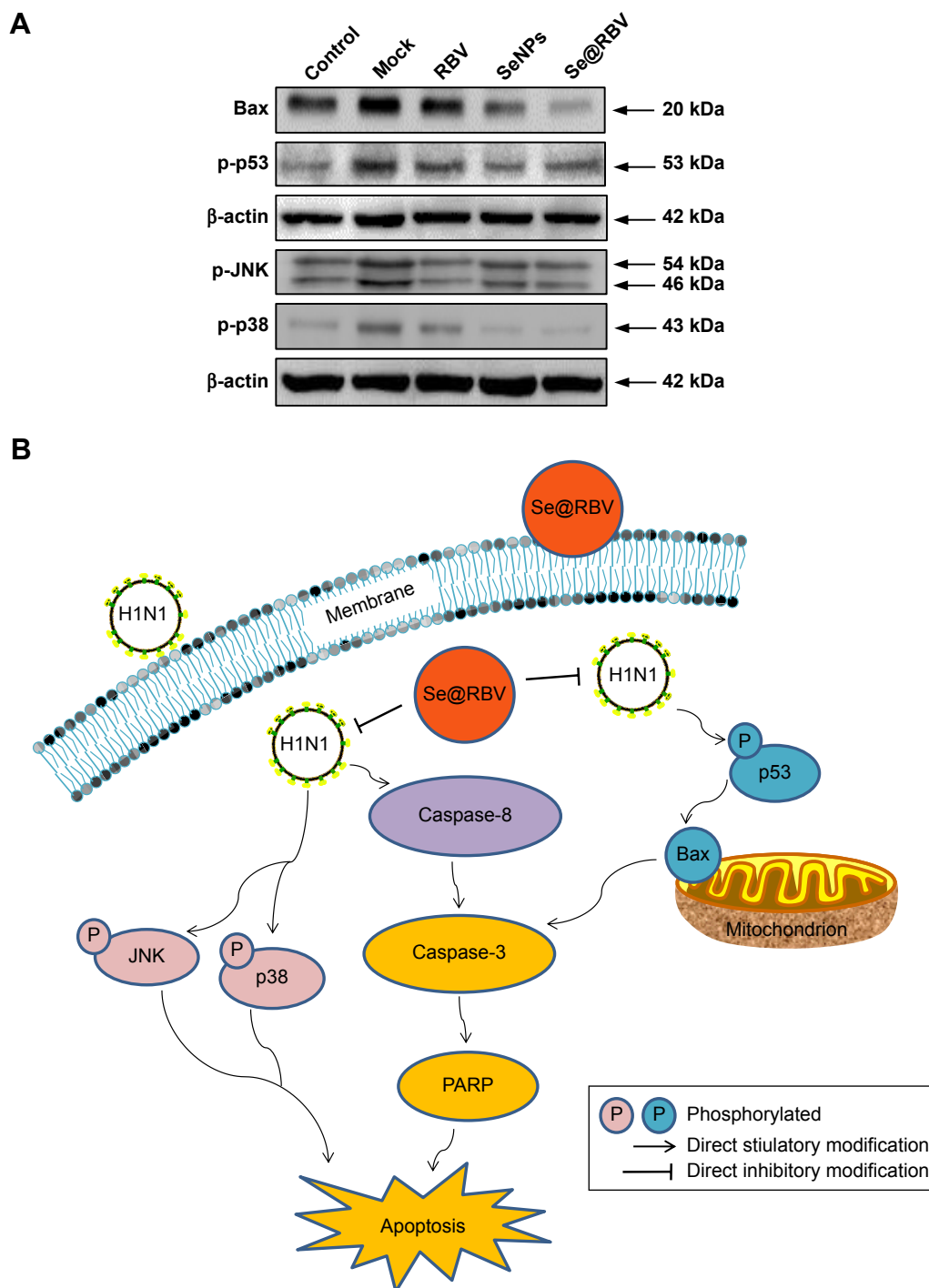
A

B

Figure 5 Inhibition of apoptosis signaling pathways in vitro.
Notes: MDCK cells infected with H1N1 virus were untreated (Mock) or treated with RBV, SeNPs, and Se@RBV for 48 hours. Cells without infection and treatment were performed as control. (**A**) Inhibition of apoptotic proteins. (**B**) Scheme of apoptosis signaling pathways.
Abbreviations: MDCK, Madin-Darby Canine Kidney; PARP, poly-ADP-ribose polymerase ; p-JNK, Jun-amino-terminal kinase; p38, phosphorylated 38; p53, phosphorylated 53; RBV, ribavirin; SeNPs, selenium nanoparticles; Se@RBV, SeNPs loaded with RBV.

the activation of caspase-8. It was shown in Figure 5B that both the regulation of caspase-8 and Bax resisted the activation of caspase-3 and inhibited apoptosis of cells.

JNK and p38 signalings could be activated by virus infection.[46] Phosphorylation of JNK or p38 is a sign of apoptosis. These two proteins were investigated in this study.

As displayed in Figure 5A, expressions of p-JNK and p-p38 increased in cells infected by H1N1 virus without subsequent treatments, but evidently decreased followed by treatment with Se@RBV. The result reflected that p38 and JNK signaling pathways took part in the restriction of apoptosis with Se@RBV.

In vivo antiviral efficiency

To evaluate the efficiency of Se@RBV against H1N1 influenza virus in vivo, mice were infected with H1N1 virus and treated with RBV, SeNPs, and Se@RBV, followed by H&E staining, tunel analyses, and immunohistochemical test of lung tissues after being executed (Figure 6A). Mice infected with H1N1 virus without other treatments tended to reduce physical activity and feeding. Mice treated with Se@RBV post infection present a more active and increased appetite. As the H&E staining reveals in Figure 6B, the H1N1-infected group manifested as alveolar collapse and perivascular and peribronchiolar edema, compared with the control group. When treated with RBV or SeNPs, the symptoms lessened. Crucially, it is quite amazing that Se@RBV attenuated the histopathological manifestations substantially. The result directly indicated that Se@RBV evidently protected the lungs from being injured by H1N1 infection. DNA around nucleosomes was cut when apoptosis occurs. Tunel is used for detecting the DNA fragmentation disrupted during apoptosis. As shown in Figure 6B, Se@RBV prevents DNA damage during H1N1 infection. Altogether, the H&E stain

and tunel analyses illustrate that Se@RBV had a good effect on lung injury in mice suffering from H1N1 virus infection. To further investigate the probable mechanism through which Se@RBV cured the mice, immunohistochemical test of the lungs was implemented. As exhibited in Figure 6C, cleaved caspase-3, cleaved PARP, p-p53, p-JNK, and p-p38 proteins were found positive for H1N1 virus infection. Nevertheless, treatment with Se@RBV reduced the appearance visibly. This result was coincident with the previous in vitro study in which caspase-3, p53, JNK, and p38 participated in the restriction against the H1N1 virus infection of Se@RBV.

Conclusion

Loaded with RBV, a broad-spectrum antiviral agent, SeNPs were prepared through a simple and highly efficient method. SeNPs modified with RBV (Se@RBV) rescued cells from apoptosis induced by H1N1 influenza virus infection and reduced the virus titer of the culture supernatant. Besides, lung injury and DNA damage were attenuated by Se@RBV treatment in mice. Furthermore, activation of caspase-3 signaling pathway was resisted by both in vitro and in vivo
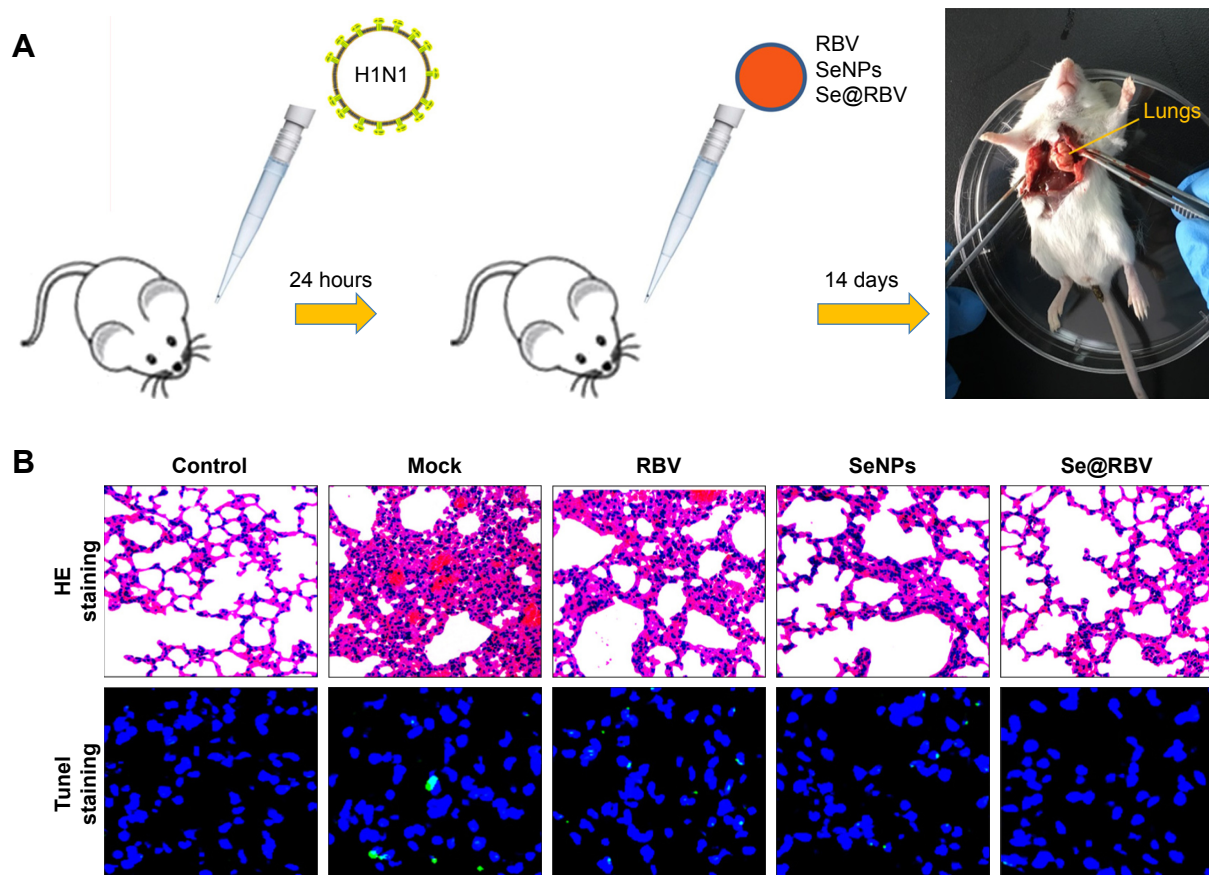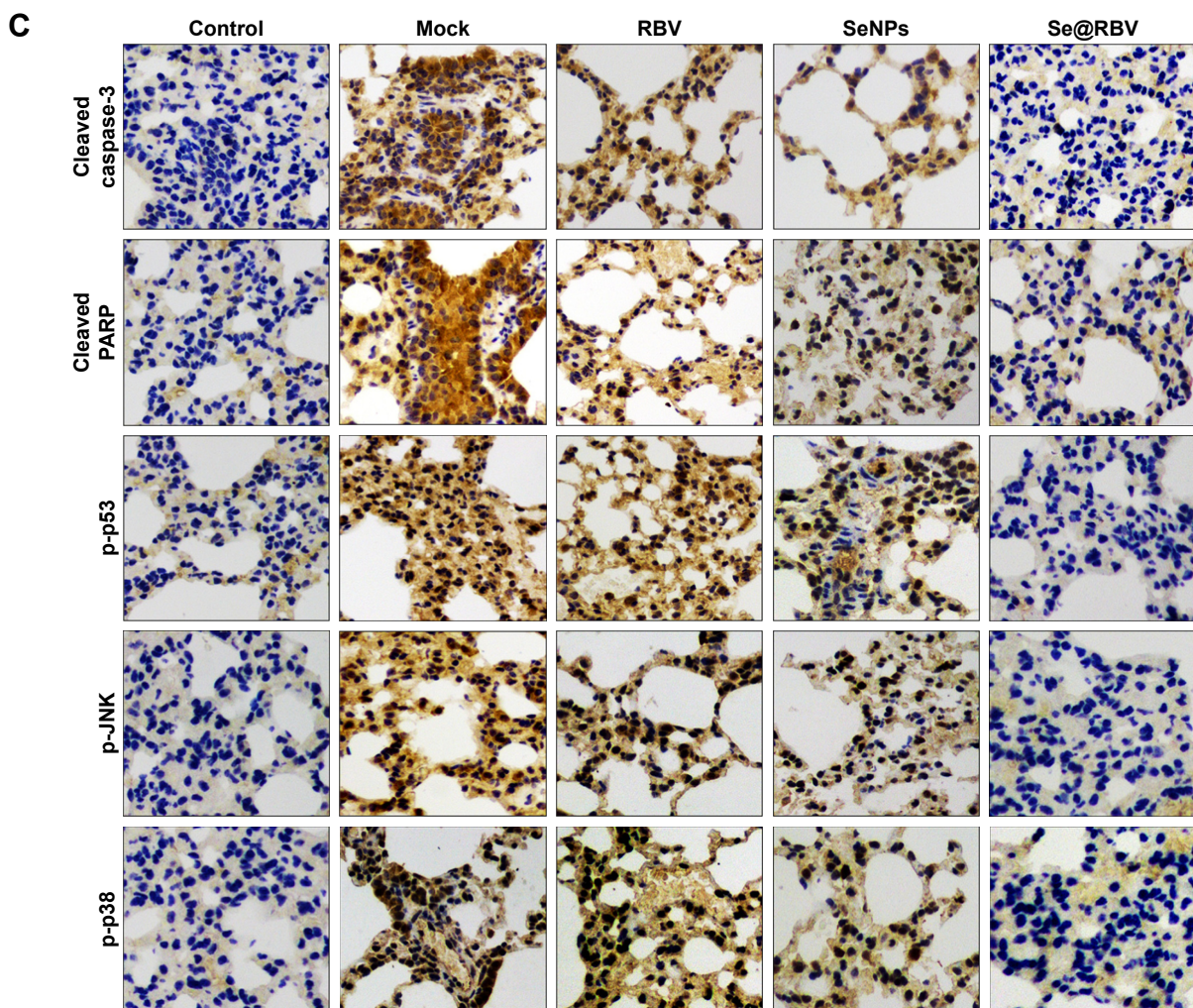

Figure 6 (*Continued*)

Figure 6 In vivo antiviral efficiency of Se@RBV.

Notes: Mice infected by H1N1 virus was treated with physiological saline (Mock), RBV, SeNPs, or Se@RBV (**A**). Mice without infection and treated with physiological saline were performed as control. H&E and tunel staining (**B**), as well as immunohistochemistry (**C**), was carried out.

Abbreviations: H&E, hematoxylin and eosin; MDCK, Madin-Darby Canine Kidney; PARP, poly-ADP-ribose polymerase; p-JNK, Jun-amino-terminal kinase; p38, phosphorylated 38; p53, phosphorylated 53; RBV, ribavirin; SeNPs, selenium nanoparticles; Se@RBV, SeNPs loaded with RBV.

experiments. In conclusion, this study elaborates that SeNPs loaded with RBV restrain apoptosis induced by H1N1 influenza virus infection through the caspase-3 signaling pathway.

Disclosure

The authors report no conflicts of interest in this work.

References

1. Lin ZF, Zhao MQ, Guo M, et al. The Seroprevalence of Some Pathogen Specific IgM in Children with Acute Respiratory Tract Infections in Guangzhou Region, 2011–2012. *Clin Lab*. 2015;61(8):917–924.
2. Zhao MQ, Wang LH, Lian GW, et al. The serum value of NO and IL-17 were increased in children with influenza A viral pneumonia. *Clin Lab*. 2015;61(10):1415–1421.
3. Rahman M, Hoque SA, Islam MA, Rahman SR. Molecular analysis of amantadine-resistant influenza A (H1N1 pdm09) virus isolated from slum dwellers of Dhaka, Bangladesh. *Virus Genes*. 2017;53(3): 377–385.

4. Li F, Ma C, Hu Y, Wang Y, Wang J, Cl M, Ym H. Discovery of potent antivirals against amantadine-resistant influenza A viruses by targeting the M2-S31N proton channel. *ACS Infect Dis*. 2016;2(10): 726–733.

5. Hussain M, Galvin HD, Haw TY, Nutsford AN, Husain M. Drug resistance in influenza A virus: the epidemiology and management. *Infect Drug Resist*. 2017;10:121–134.

6. Nykvist M, Gillman A, Söderström Lindström H, et al. In vivo mallard experiments indicate that zanamivir has less potential for environmental influenza A virus resistance development than oseltamivir. *J Gen Virol*. 2017;98:2937–2949.

7. Liao SH, Li Y, Lai YN, Liu N, Zhang FX, Xu PP. Ribavirin attenuates the respiratory immune responses to influenza viral infection in mice. *Arch Virol*. 2017;162(6):1661–1669.

8. Westover JB, Sefing EJ, Bailey KW, et al. Low-dose ribavirin potentiates the antiviral activity of favipiravir against hemorrhagic fever viruses. *Antiviral Res*. 2016;126:62–68.

9. de Souza E Silva JM, Hanchuk TD, Santos MI, Kobarg J, Bajgelman MC, Cardoso MB. Viral inhibition mechanism mediated by surface-modified silica nanoparticles. *ACS Appl Mater Interfaces*. 2016;8(26):16564–16572.

10. Yang Y, Xie Q, Zhao Z, et al. Functionalized Selenium Nanosystem as Radiation Sensitizer of ^{125}I Seeds for Precise Cancer Therapy. *ACS Appl Mater Interfaces*. 2017;9(31):25857–25869.

11. Li Y, Guo M, Lin Z, et al. Polyethylenimine-functionalized silver nanoparticle-based co-delivery of paclitaxel to induce HepG2 cell apoptosis. *Int J Nanomedicine*. 2016;11:6693–6702.

12. Singh P, Pandit S, Mokkapati V, Garg A, Ravikumar V, Mijakovic I. Gold Nanoparticles in Diagnostics and Therapeutics for Human Cancer. *Int J Mol Sci*. 2018;19(7):1979.

13. Yue J, Luo SZ, Lu MM, Shao D, Wang Z, Dong WF. A comparison of mesoporous silica nanoparticles and mesoporous organosilica nanoparticles as drug vehicles for cancer therapy. *Chem Biol Drug Des*. 2018;92(2):1435–1444.

14. Steinbrenner H, Al-Quraishy S, Dkhil MA, Wunderlich F, Sies H. Dietary selenium in adjuvant therapy of viral and bacterial infections. *Adv Nutr*. 2015;6(1):73–82.

15. Kamwesiga J, Mutabazi V, Kayumba J, et al. Effect of selenium supplementation on CD4+ T-cell recovery, viral suppression and morbidity of HIV-infected patients in Rwanda: a randomized controlled trial. *AIDS*. 2015;29(9):1045–1052.

16. Ivory K, Prieto E, Spinks C, et al. Selenium supplementation has beneficial and detrimental effects on immunity to influenza vaccine in older adults. *Clin Nutr*. 2017;36(2):407–415.

17. Cheng Z, Zhi X, Sun G, et al. Sodium selenite suppresses hepatitis B virus transcription and replication in human hepatoma cell lines. *J Med Virol*. 2016;88(4):653–663.

18. Mahdavi M, Mavandadnejad F, Yazdi MH, et al. Oral administration of synthetic selenium nanoparticles induced robust Th1 cytokine pattern after HBs antigen vaccination in mouse model. *J Infect Public Health*. 2017;10(1):102–109.

19. Ramya S, Shanmugasundaram T, Balagurunathan R. Biomedical potential of actinobacterially synthesized selenium nanoparticles with special reference to anti-biofilm, anti-oxidant, wound healing, cytotoxic and anti-viral activities. *J Trace Elem Med Biol*. 2015;32:30–39.

20. Li Y, Lin Z, Guo M, et al. Inhibitory activity of selenium nanoparticles functionalized with oseltamivir on H1N1 influenza virus. *Int J Nanomedicine*. 2017;12:5733–5743.

21. Li Y, Lin Z, Guo M, et al. Inhibition of H1N1 influenza virus-induced apoptosis by functionalized selenium nanoparticles with amantadine through ROS-mediated AKT signaling pathways. *Int J Nanomedicine*. 2018;13:2005–2016.

22. Choi JH, Jeong H, Jang KL. Hepatitis B virus X protein suppresses all-trans retinoic acid-induced apoptosis in human hepatocytes by repressing p14 expression via DNA methylation. *J Gen Virol*. 2017;98(11): 2786–2798.

23. Afroz S, Garg R, Fodje M, van Drunen Littel-van den Hurk S. The Major Tegument Protein of Bovine Herpesvirus 1, VP8, Interacts with DNA Damage Response Proteins and Induces Apoptosis. *J Virol*. 2018;92(15):e00773–18.

24. Dw L, Zhang K, Li R. Interferon regulatory factor 8 regulates caspase-1 expression to facilitate Epstein-Barr virus reactivation in response to B cell receptor stimulation and chemical induction. *PLoS Pathog*. 2018; 14(1):e1006868.

25. Shang N, Bank T, Ding X, et al. Caspase-3 suppresses diethylnitrosamine-induced hepatocyte death, compensatory proliferation and hepatocarcinogenesis through inhibiting p38 activation. *Cell Death Dis*. 2018;9(5):558–568.

26. Li Y, Lin Z, Zhao M, et al. Multifunctional selenium nanoparticles as carriers of HSP70 siRNA to induce apoptosis of HepG2 cells. *Int J Nanomedicine*. 2016;11:3065–3076.

27. Lin Z, Li Y, Guo M, et al. The inhibition of H1N1 influenza virus-induced apoptosis by silver nanoparticles functionalized with zanamivir. *RSC Adv*. 2017;7(2):742–750.

28. Li Y, Lin Z, Zhao M, et al. Silver nanoparticle based codelivery of oseltamivir to inhibit the activity of the H1N1 influenza virus through ROS-mediated signaling pathways. *ACS Appl Mater Interfaces*. 2016; 8(37):24385–24393.

29. Bae JY, Lee I, Kim JI, et al. A Single Amino Acid in the Polymerase Acidic Protein Determines the Pathogenicity of Influenza B Viruses. *J Virol*. 2018;92(13):e00259-18.

30. Qu M, Ding F, di S, Zhang S, Yu X. The Effects of Epstein-Barr Virus Nuclear Antigen 2 (EBNA2) on B-Lymphocytic Activity. *Clin Lab*. 2018; 64(4):425–431.

31. Lin Z, Li Y, Guo M, et al. Inhibition of H1N1 influenza virus by selenium nanoparticles loaded with zanamivir through p38 and JNK signaling pathways. *RSC Adv*. 2017;7(56):35290–35296.

32. Zhu B, Li Y, Lin Z, et al. Silver Nanoparticles Induce HePG-2 Cells Apoptosis Through ROS-Mediated Signaling Pathways. *Nanoscale Res Lett*. 2016;11(1):198.

33. Liu XY, Zhang FR, Shang JY, et al. Renal inhibition of miR-181a ameliorates 5-fluorouracil-induced mesangial cell apoptosis and nephrotoxicity. *Cell Death Dis*. 2018;9(6):610–623.

34. du T, Liang J, Dong N, et al. Glutathione-Capped Ag$_2$S Nanoclusters Inhibit Coronavirus Proliferation through Blockage of Viral RNA Synthesis and Budding. *ACS Appl Mater Interfaces*. 2018;10(5): 4369–4378.

35. Lee ACY, To KKW, Zhang AJX, et al. Triple combination of FDA-approved drugs including flufenamic acid, clarithromycin and zanamivir improves survival of severe influenza in mice. *Arch Virol*. Epub 2018 May 7.

36. Chida J, Hara H, Yano M, et al. Prion protein protects mice from lethal infection with influenza A viruses. *PLoS Pathog*. 2018;14(5):e1007049.

37. Xia Y, Lin Z, Li Y, et al. Targeted delivery of siRNA using RGDfC-conjugated functionalized selenium nanoparticles for anticancer therapy. *J Mater Chem B*. 2017;5(33):6941–6952.

38. Chauhan P, Sheng WS, Hu S, Prasad S, Lokensgard JR. Nitrosative damage during retrovirus infection-induced neuropathic pain. *J Neuroinflammation*. 2018;15(1):66–81.

39. Zhu B, Xu T, Lin Z, et al. Recombinant heat shock protein 78 enhances enterovirus 71 propagation in Vero cells and is induced in SK-N-SH cells during the infection. *Arch Virol*. 2017;162(6):1649–1660.

40. Jiang W, Fu Y, Yang F, et al. Gracilaria lemaneiformis polysaccharide as integrin-targeting surface decorator of selenium nanoparticles to achieve enhanced anticancer efficacy. *ACS Appl Mater Interfaces*. 2014; 6(16):13738–13748.

41. Yh L, Lin ZF, Zhao MQ, et al. Reveral of H1N1 influenza virus-induced apoptosis by silver nanoparticles functionalized with amantadine. *RSC Adv*. 2016;6:89679–89686.

42. Sobrido-Cameán D, Barreiro-Iglesias A. Role of caspase-8 and Fas in cell death after spinal cord injury. *Front Mol Neurosci*. 2018;11:101.

43. Song F, Yu X, Zhong T, et al. Caspase-3 inhibition attenuates the cytopathic effects of EV71 infection. *Front Microbiol*. 2018;9:817.

44. Haddadi R, Nayebi AM, Eyvari Brooshghalan S. Silymarin prevents apoptosis through inhibiting the Bax/caspase-3 expression and suppresses toll like receptor-4 pathway in the SNc of 6-OHDA intoxicated rats. *Biomed Pharmacother*. 2018;104:127–136.

45. Beberok A, Wrześniok D, Rok J, et al. Ciprofloxacin triggers the apoptosis of human triple-negative breast cancer MDA-MB-231 cells via the p53/Bax/Bcl-2 signaling pathway. *Int J Oncol*. 2018;52(5): 1727–1737.

46. Wang L, Song LF, Chen XY, et al. MiR-181b inhibits P38/JNK signaling pathway to attenuate autophagy and apoptosis in juvenile rats with kainic acid-induced epilepsy via targeting TLR4. *CNS Neurosci Ther*. Epub 2018 May 28.